Hacettepe Journal of Mathematics and Statistics
Volume 44 (6) (2015), 1445 – 1462

Effect of hall current on the MHD fluid flow and heat transfer due to a rotating disk with uniform radial electric field

Nihan Uygun*

Abstract

In this paper the steady Von Kármán flow of incompressible fluid in which the Hall effect exists is analyzed over the infinite rotating disk with additional assumptions: the uniform magnetic field applied normally to the disk and the radial electric field imposed to the disk. Therefore, the stability equations and energy equation have been modified in the presence of Hall effect, uniform magnetic field and radial electric field. The system of equations generated by stability and energy equations has been solved using Chebyshev collocation technique for varying values of Hall parameters, magnetic interaction and radial electric parameters. Accuracy of the method is verified comparing results in the literature. Effects of parameters are depicted graphically and are analyzed.

Keywords: Incompressible Flow, Rotating-Disk flow, Magnetic field, Electric field, Hall effect.

2000 AMS Classification: 76W05

Received : 21.05.2014 *Accepted* : 09.09.2014 *Doi* : 10.15672/HJMS.2015449675

1. Introduction

Rotating disk flow has been extensively studied in the literature. An interesting problem from both engineering and mathematical point of view has been investigated for the last half of the century using experimental, analytical and numerical means. Rotating disk flows are important in many applications such as turbomachinery, oceanography, computer storage devices, nuclear reactors, lubrication, and so on.

Von Kármán [13] has carried out the pioneering study of fluid flow, triggered further studies, many explanations are initiated on infinite rotating disk. Cochran [7] and Benton [5] have considered by Kármán [13], they investigated the steady motion of an incompressible viscous fluid. The effect of uniform magnetic field on the flow over a rotating infinite disk has been studied by many researchers [8], [12], [19], [20], [22], [23], [24], [25]. Hall effect has been taken into consideration in some of the works in the literature. To the best of our knowledge Attia[2] has initiated in his studies examining Hall effect on the flow over a infinite rotating disk. The study has been followed by Attia & Aboul-Hassan[1], and Siddiqui, Rana & Naseer[19]. The case without Hall effect on the rotating infinite disk has been investigated [4], [6], [8], [9], [12], [14], [15], [16], [19], [20], [21], [22], [23], [24], [25].

Millsaps & Pohlhausen[15] have considered the heat transfer problem on the rotating infinite disk. After their work, the heat transfer on a flat plate was analyzed by Sparrow

*Mathematics Department, University of Abant Izzet Baysal,Bolu/Turkey.
Email : nuygun@ibu.edu.tr

& Gregg[21] for Prandtl numbers. Sparrow & Cess[20], Riley[16], Kumar & Thacker & Watson[14] studied the effects of magnetic field to the heat transfer over a infinite rotating disk. Finally, effects of the uniform radial electric field on the MHD heat and fluid flow due to a rotating disk was investigated by Turkyilmazoglu[22].

In most of the studies, the Hall term is neglected for small or moderate values of the magnetic field in applying Ohm's law in the analysis. When a strong magnetic field is applied, the influence of electromagnetic force is noticeable as stated by Cramer and Pai [8]. Therefore, the Hall current is important and it has a marked effect on the magnitude and direction of the current density and consequently on the magnetic force term.

In this work, following the above approach, steady hydromagnetic flow of viscous, incompressible fluid over rotating infinite disk is examined with the radial electric field taking Hall effect into consideration. An external uniform magnetic field is imposed on the normal direction. The radial electric field is produced by electric potential. In the rotating infinite disk, the magnetic Reynolds number is assumed to be very small. Navier-Stokes equations and energy equation are solved by using Chebyshev collocation method. The effects of Hall parameters, magnetic field and electric field are analyzed.

2. Basic Equations

Let us consider the three-dimensional steady viscous incompressible conducting fluid over infinite rotating disk. The disk is assumed to be rotating about z-axis with a constant angular velocity Ω in the cylindrical coordinates (r, θ, z). An external uniform magnetic field is applied in the z-direction and has a constant magnetic flux density B_0. The magnetic Reynolds number is assumed to be very small, therefore, the effect on the imposed magnetic field is negligible. The disk is taken electrically conducting with $e = (e_r, e_\theta, e_z)$ denoting the electric field, in which $e_\theta = 0$ due to axisymmetric flow assumption, by the work of Kármán [13]. Moreover, the effect of uniform electric field on the disk flow is produced by electrical potential is given by $e_r = -B_0\Omega\gamma r$ [10]. In magnetic field, the electric current can be written by Ohm's law $j = \sigma(e + \mathbf{v} \times B - \beta(j \times B))$ where $j = (j_r, j_\theta, j_z)$ is the current density vector, σ is the electrical conductivity, and the last term defines the Hall effect as β is the Hall factor. The disk flow motion is governed by Maxvell's equation, continuity equation, the Navier-Stokes equations including the Lorentz force as follows

$$\nabla \cdot j = 0, \tag{2.1}$$

$$\nabla \cdot \mathbf{v} = 0, \tag{2.2}$$

$$\rho\big[\frac{\partial \mathbf{v}}{\partial t} + (\mathbf{v} \cdot \nabla)\mathrm{v}\big] = -\nabla p + \frac{1}{Re}\big[\nabla^2 \mathbf{v}\big] + M_n(j \times B)_i \tag{2.3}$$

Lorentz force terms $M_n(j \times B)_i$ represents the existence of magnetic field in the fluid motion equations. The presence of the force, originating from magnetic field, on the flow of conducting fluids can alter the velocity and pressure characteristics of the flow.

In general Maxwell's equation is defined by

$$\nabla \times e = -\frac{\partial B}{\partial t}. \tag{2.4}$$

In the case of time-independent flow, the equation(2.4) is turned into the equation below,

$$\nabla \times e = 0.$$

Therefore, there is a conservative electric field which arises by electric potential Φ, arriving to $e = -\nabla\Phi$.

Several parameters appearing in equations (2.1-2.3) are defined as follows, ρ is the density, $\mathbf{v} = (u, v, w)$ is the velocity vector, ∇ is the usual gradient operator in cylindrical coordinates, p is the pressure, Re is the Reynolds number characterizing the flow defined by $Re = \frac{\Omega}{\nu}$, ν is the kinematic viscosity of the fluid. Finally M_n is the magnetic interaction parameter, which represents the ratio between the magnetic force and the fluid

inertia force. In component form of Maxvell's equation, continuity equation and momentum equations with Lorentz force can be written as

$$\frac{\partial j_r}{\partial r} + \frac{\partial j_z}{\partial z} + \frac{j_r}{r} = 0, \tag{2.5}$$

$$\frac{\partial u}{\partial r} + \frac{\partial w}{\partial z} + \frac{w}{r} = 0, \tag{2.6}$$

$$u\frac{\partial u}{\partial r} + w\frac{\partial u}{\partial z} - \frac{v^2}{r} = -\frac{\partial p}{\partial r} + \frac{1}{Re}\left[\nabla^2 u - \frac{u}{r^2}\right] + \frac{M_n}{1+m^2}\left[me_r - u + mv\right], \tag{2.7}$$

$$u\frac{\partial v}{\partial r} + w\frac{\partial v}{\partial z} + \frac{uv}{r} + 2u = \frac{1}{Re}\left[\nabla^2 v - \frac{v}{r^2}\right] + \frac{M_n}{1+m^2}\left[-e_r - mu - v\right], \tag{2.8}$$

$$u\frac{\partial w}{\partial r} + w\frac{\partial w}{\partial z} = -\frac{\partial p}{\partial z} + \frac{1}{Re}\left[\nabla^2 w\right], \tag{2.9}$$

where $m = \sigma\beta B_0$ is the Hall parameter. The Hall parameter can take any value. In case of positive values of m, B_0 is upwards and the electrons of the conducting fluid gyrate in the same sense as the rotating disk. On the other hand, when m takes negative values, B_0 is downwards and the electrons gyrate in an opposite sense to the disk.

In equations(2.7-2.8), Lorentz force terms are $j \times B = B_0(j_\theta, -j_r, 0)$, and the components of current density vector are easily derived by Ohm's law as

$$(j_r, j_\theta, j_z) = \frac{\sigma}{1+m^2}\left(e_r + mu + v, me_r - u + mv, (1+m^2)e_z\right).$$

Because of imposing radial electric field in velocity at infinity, the tangential direction velocity is given by $v = \Omega\gamma r$. Furthermore, existence of potential flow due to radial electric field at the edge of the boundary layer implies that pressure gradient in the radial direction is $\frac{\partial p}{\partial r} = \rho\Omega^2\gamma^2 r$ (see Evans[10]). When these are taken into consideration, boundary conditions become

$$\begin{array}{llll} u = 0, & v = r\Omega, \quad w = 0, \quad j_z = 2r\Omega B_0 C\gamma, & \text{at} \quad z = 0, \\ u \to 0, & v \to r\Omega\gamma, & \text{as} \quad z \to \infty, \end{array} \tag{2.10}$$

where C is the wall conduction ratio of the electrical conductance of the wall to electrical conductivity of the fluid.

The basic flow of incompressible case, which is also called as Von Kármán's steady state flow is well known. The Von Kármán's[13] flow will be considered here, which means that the disk flow is assumed to evolve alongside the boundary layer coordinate $\eta = Re^{1/2}z$, in conformity with the self similarity variables (see Hossain,Hossain& Wilson[11])

$$\begin{array}{l} (u, v, w, p) = (r\Omega F(\eta), r\Omega G(\eta), Re^{-1/2}H(\eta), \rho\Omega^2 P(\eta)), \\ (j_r, j_\theta, j_z) = (B_0 r\Omega J_r(\eta), B_0 r\Omega J_\theta(\eta), B_o\Omega Re^{-1/2} J_z(\eta)), \\ (e_r, e_\theta, e_z) = (B_0 r\Omega E_r(\eta), 0, B_0\Omega Re^{-1/2} E_z(\eta)). \end{array} \tag{2.11}$$

These quantities substitute into the governing equations (2.5-2.9), and also neglect terms of $O(Re^{-1})$, the disk flow quantities are determined from the subsequent equations and boundary conditions(2.10) as

$$2J_r + J_z' = 0, \tag{2.12}$$

$$2F + H' = 0, \tag{2.13}$$

$$F^2 - G^2 + F'H - F'' - \frac{M_n}{1+m^2}\left[-m\gamma - F + mG\right] + \gamma^2 = 0, \tag{2.14}$$

$$2FG + G'H - G'' - \frac{M_n}{1+m^2}\left[\gamma - G - mF\right] = 0, \tag{2.15}$$

$$P' + H'H - H'' = 0, \tag{2.16}$$

$$\begin{array}{llll} F = 0, & G = 1, \quad H = 0, \quad J_z = 2C\gamma & \text{at} \quad \eta = 0, \\ F \to 0, & G \to \gamma & \text{as} \quad \eta \to \infty, \end{array} \tag{2.17}$$

a prime denotes derivative with respect to η. The initial and boundary conditions(3.3) show the no-slip boundary conditions of governing equations at the surface of disk and a far field disk flow, respectively.

3. Analysis of the Heat Transfer

Due to the difference in the temperature between the surface of the disk and the ambient fluid, heat transfer takes place. The energy equation, with viscous dissipation and Joule heating depending on the Hall effect, takes the form

$$\begin{aligned}\rho\big[\tfrac{\partial T}{\partial t} \quad &+(\mathbf{v}\cdot\nabla)T\big] = M_\infty^2(\Gamma-1)\big[\tfrac{\partial p}{\partial t}+(\mathbf{v}\cdot\nabla)p\big] + \tfrac{1}{Pr}\tfrac{1}{Re}\big[\nabla^2 T\big]\\ &+\tfrac{\Gamma-1}{Re}M_\infty^2\big[\Phi\big] + M_n(\Gamma-1)M_\infty^2\tfrac{j^2}{\sigma}\end{aligned} \tag{3.1}$$

where T is the temperature of the fluid, $Pr = \frac{\mu c_p}{k}$ is the Prandtl number c_p is the specific heat capacity, μ is the dynamical viscosity and k is thermal conductivity of the fluid. Moreover, Γ is the ratio of the specific heats, M_∞ is the free stream Mach number. Finally, the last two terms in the right-hand-side of Eq.(3.1) represent

$$\Phi = (\frac{\partial u}{\partial z})^2 + (\frac{\partial v}{\partial z})^2,$$

the viscous dissipation and

$$\frac{j^2}{\sigma} = \frac{1}{(1+m^2)^2}\big[(e_r+mu+v)^2 + (me_r-u+mv)^2 + (1+m^2)^2 e_z^2\big]$$

Joule heating terms respectively.

Using the Von Kármán [13] assumptions, similarities of (2.11) and also neglecting terms of $O(Re^{-1})$, equation(3.1) becomes

$$\begin{aligned}\tfrac{1}{Pr}T'' \quad &-HT' + M_\infty^2(\Gamma-1)\big[\gamma^2 F + F'^2 + G'^2\big]\\ &+M_\infty^2(\Gamma-1)\tfrac{M_n}{(1+m^2)^2}\big[(-\gamma+mF+G)^2 + (-m\gamma-F+mG)^2\big] = 0,\end{aligned} \tag{3.2}$$

and the initial and boundary conditions for the energy equation are

$$\begin{aligned} T &= T_w, \qquad &\text{at} \quad \eta = 0,\\ T &\to T_\infty, \qquad &\text{as} \quad \eta \to \infty,\end{aligned} \tag{3.3}$$

recalling that a prime indicates derivative in term of η. In the last two equations, T_w is the temperature at the surface of the disk, T_∞ is the temperature of the ambient fluid at a large distance from the disk. Introducing the non-dimensional variable $\theta = \frac{T-T_\infty}{T_w-T_\infty}$, the equation(3.2), the initial and boundary conditions(3.3) take the forms

$$\begin{aligned}\tfrac{1}{Pr}\theta'' \quad &-H\theta' + E_c\big[\gamma^2 F + F'^2 + G'^2\big]\\ &+\tfrac{M_n E_c}{(1+m^2)^2}\big[(-\gamma+mF+G)^2 + (-m\gamma-F+mG)^2\big] = 0,\end{aligned} \tag{3.4}$$

$$\begin{aligned} \theta &= 0, \qquad &\text{at} \quad \eta = 0,\\ \theta &\to 1, \qquad &\text{as} \quad \eta \to \infty,\end{aligned} \tag{3.5}$$

where $E_c = \frac{M_\infty^2(\Gamma-1)}{T_w-T_\infty}$ is the Eckert number. The heat transfer from the disk surface to the fluid is computed by the application of the Fourier's law, and using transformation for heat term we have

$$\begin{aligned} q &= -k\left(\tfrac{\partial T}{\partial z}\right)_w\\ &= -k(T_w-T_\infty)\sqrt{\tfrac{\Omega}{\nu}}\tfrac{d\theta(0)}{d\eta},\end{aligned} \tag{3.6}$$

by rephrasing the heat transfer result in terms of the Nusselt number, defined as

$$N_u = \frac{q\sqrt{\frac{\nu}{\Omega}}}{k(T_w-T_\infty)}$$

Therefore the second part of the equation (3.6) turns into

$$N_u = -\frac{d\theta(0)}{d\eta} \tag{3.7}$$

The action of viscosity in the fluid adjacent to the disk tends to set up tangential shear stress, which opposes the rotation of the disk. There is also a surface shear stress in the radial direction. Consequently, it is necessary to provide a torque at the shaft to maintain a steady rotation. Applying the Newtonian formula, the radial component τ_r and tangential component τ_θ of the shear stress are respectively expressed by

$$\tau_r = \left(\frac{\partial u}{\partial z}\right)_w = r\Omega\sqrt{\frac{\Omega}{\nu}}F'(0) \tag{3.8}$$

$$\tau_\theta = \left(\frac{\partial v}{\partial z}\right)_w = r\Omega\sqrt{\frac{\Omega}{\nu}}G'(0) \tag{3.9}$$

Of physical interest is also the magnitude of the constant axial velocity at infinity, given by $H(\infty)$ and the resisting the turning moment (or torque) T_0 on the disk of radius R

$$T_0 = -\int_0^R \mu\left(\frac{\partial v}{\partial z}\right)_w 2\pi r^2 dr = -\frac{\rho\Omega\pi}{2}\sqrt{\Omega\nu}G'(0) \tag{3.10}$$

In this study, a matrix method called Chebyshev collocation method is presented for numerical solution of the equations (2.12-2.16) and (3.3) under the initial and boundary conditions (2.17) and (3.4) respectively by a truncated Chebyshev series. Using the Chebyshev collocation points, this method transforms the differential-integral equations to a matrix equation which corresponds to a system of linear algebraic equations with unknown Chebyshev coefficients. Therefore, this allows us to use computer for solution of the equations. In addition, the Chebyshev collocation method can be used for differential and integral equations.

4. Results and Discussions

In this section, we numerically solved the system of differential equations (2.12-2.16) under the initial and boundary conditions (2.17). The energy equation (3.3) relating to the initial and boundary conditions (3.4) was calculated using velocity profiles which were given in the previous case. The numerical results were obtained by utilizing Spectral Chebyshev collocation scheme.

In many boundary layer problems different methods have been applied to solve the system of the equations. For example, Sahoo [17], Attia [2], Jasmine & Gajjar [12] and Turkyilmazoglu [22], [25] reached their results using finite-difference method, a special technique, and also Chebyshev collocation method respectively.

In this work we use spectral Chebyshev collocation scheme based on the Chebsyhev polynomials. We briefly summarize the numerical scheme as follows: Nonlinear terms are linearized with the Newton linearization technique in the given equations. Using the Chebyshev collocation points, the linearized equations are transformed to a matrix equations with unknown Chebyshev coefficients and matrix system is solved by decomposition technique.

To verify the accuracy of the numerical scheme, as well as, to validate the code, we compared our results with the outcome of the studies by Sahoo [17] and Turkyilmazoglu [22]. For comparison purpose, the results of Sahoo [17], and Turkyilmazoglu [22] are tabulated in Table 1 and Table 2, which presents a clear evidence for accuracy of the numerical method. Moreover, Figure 1, which demonstrates the velocity profiles of the generalized Von Kármán's flow for the boundary layer over the rotating disk, is given below. This figure has been included in many relevant studies, as well.

Equations (2.13-2.15) under the conditions (2.17) are solved to compute the various velocity profiles in relation with the several Magnetic interaction parameters, Hall parameters and the radial electric parameters, as depicted in Figures (2-7). It is observed that if the radial electric parameter γ becomes larger than unity, the radial velocity profile decreases as the Hall parameter increases, if not, that is, the radial electric parameter γ

M_n	$F'(0)$		$-G'(0)$	
	Present	Sahoo	Present	Sahoo
0.0	0.510232	0.510214	0.615922	0.615909

Table 1. Comparison of the numerical solutions of shear stress coefficients in radial and tangential directions $F'(0)$, $-G'(0)$ respectively.

M_n	P_r	Γ	$H(\infty)$		-$\theta'(0)$	
			Present	Turkyilmazoglu	Present	Turkyilmazoglu
0.5	1.0	0.0	-0.458880064	-0.45888005	0.282655934	0.28265593

Table 2. Comparison of numerical solutions of the vertical velocity, $H(\infty)$ and coefficients of the heat transfer, $-\theta'(0)$.

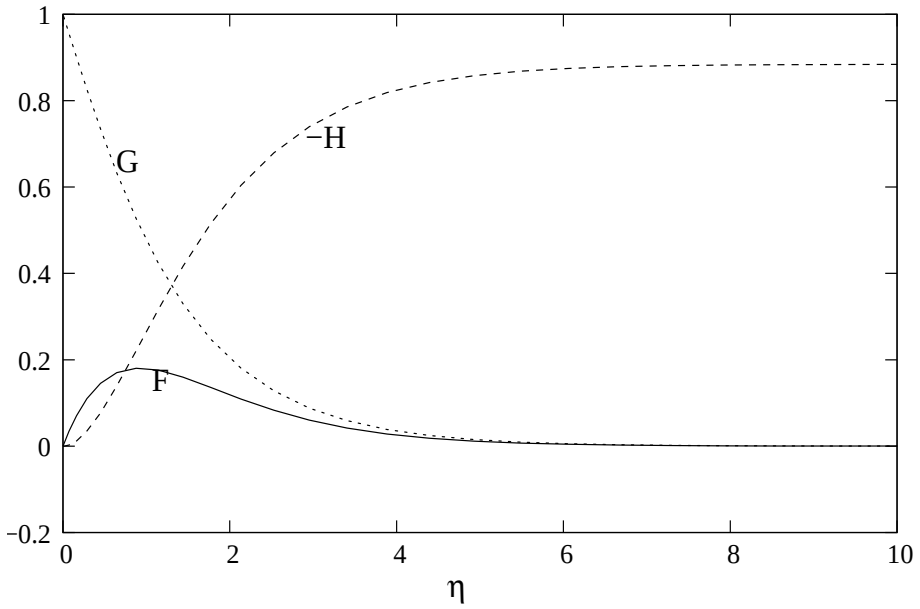

Figure 1. Velocity profiles of the generalized Von Kármán's flow are shown against the coordinate η.

gets less than unity a reverse effect takes place. It should be noted that, in both cases the size of the interval of η decreases as Hall parameter increases in Figures (2(a)-4(a)). Similarly, the size of the interval of ν decreases while a Magnetic interaction parameter increases according to graphs (2(a)-5(a)). These figures delineate that the negative Hall parameter has prominent effect on the radial component of velocity. It is interesting to find out from Figures (2(a)-7(a)) that F reverses its sign for some values of η, which proves that radial reverse flow can occur near the surface. This interesting phenomenon is interpreted as follows: the decelerated fluid particles in the boundary layer do not, in all cases, remain the thin layer which adheres to the disk along the whole wetted length of the surface. In some cases the boundary layer increases its thickness considerably in the downstream direction and the flow in the boundary layer becomes reversed. This causes the decelerated fluid particles to be forced outwards (see Schlicting[18]). Similar effect is observed in figures (2(a)-7(a)) and also in the paper by Turkyilmazoglu [22] for negative radial electric parameters.

In graphs (2(b)-7(b)), there is no meaningful change in the tangential velocity profile when the Hall parameter or the magnetic interaction parameter increases or decreases.

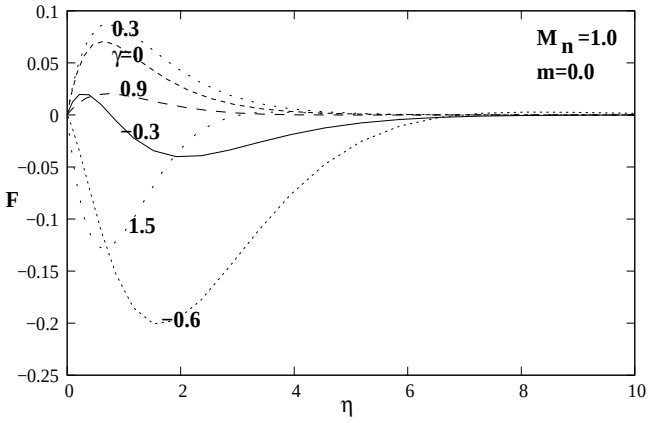

(a)

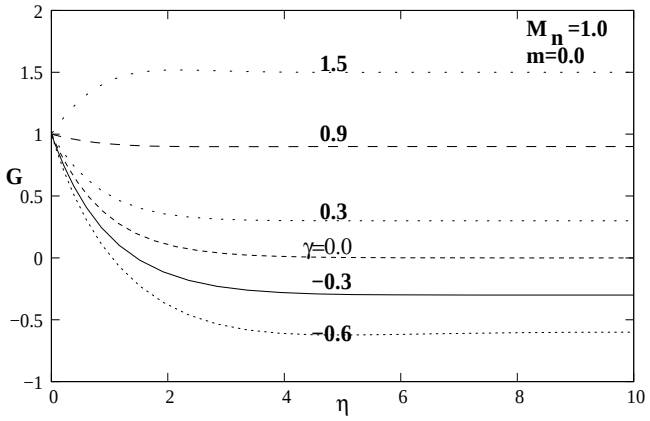

(b)

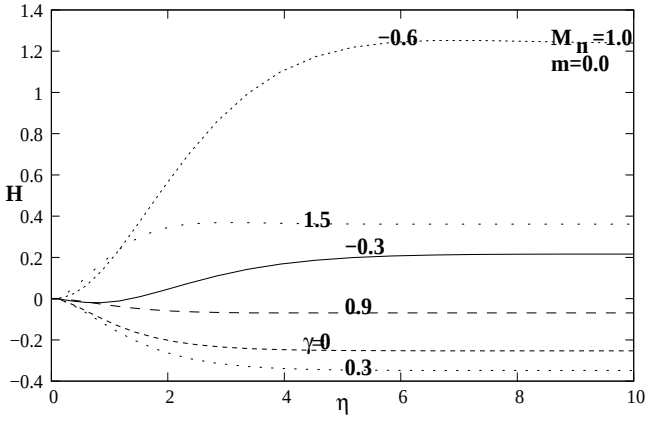

(c)

Figure 2. Velocity profiles of the generalized Von Karman's flow are shown for $M_n = 1.0$ and $m = 0.0$ at six different radial electric parameters, respectively in (a) for radial F, in (b) for tangential G, and in (c) for axial H components.

The effect of the Hall parameter on the axial component of the velocity can be visualized as in Figures (2(c)-7(c)). In case of having positive radial electric parameter values, it does

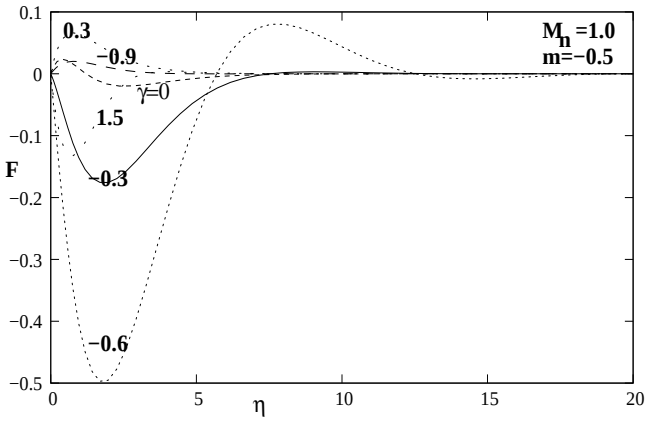

(a)

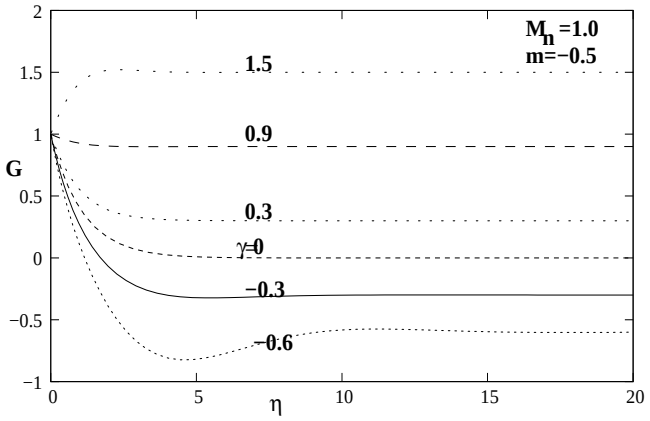

(b)

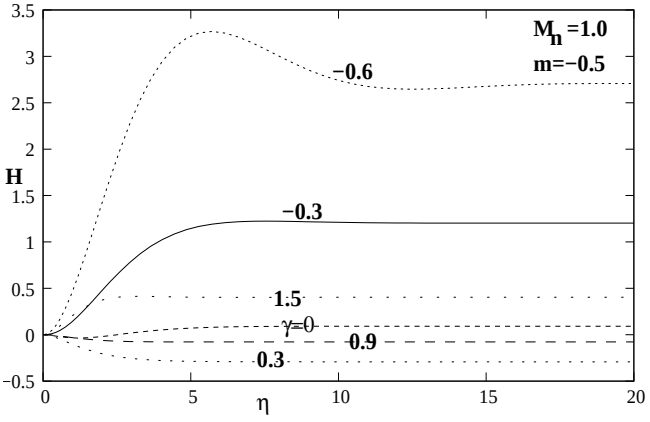

(c)

Figure 3. Velocity profiles of the generalized Von Kármán's flow are shown for $M_n = 1.0$ and $m = -0.5$ at six different radial electric parameters, respectively in (a) for radial F, in (b) for tangential G, and in (c) for axial H components.

not matter whether the change on the axial velocity profile as Hall parameter increases or decreases. On the other hand, while the radial electric parameter takes negative values, the

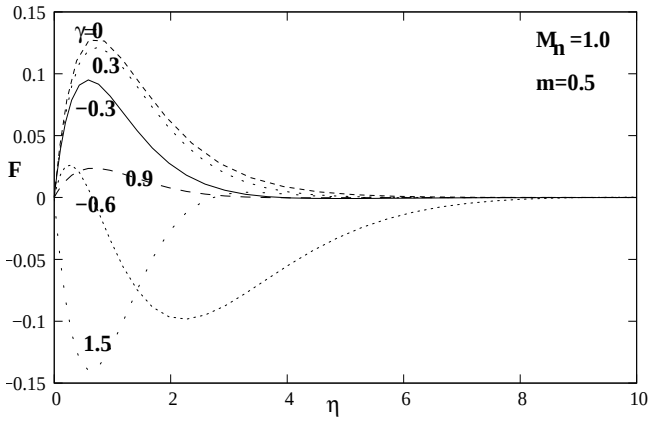

(a)

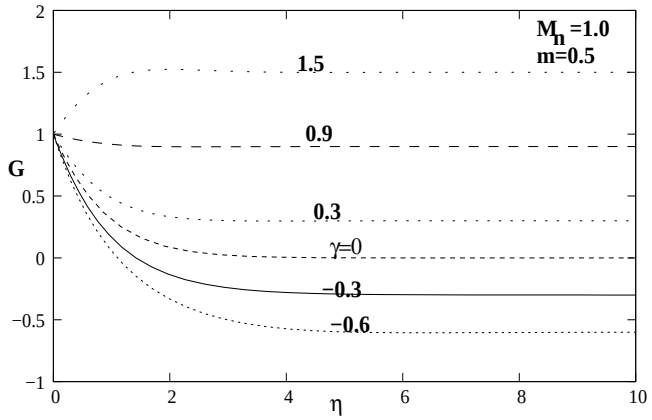

(b)

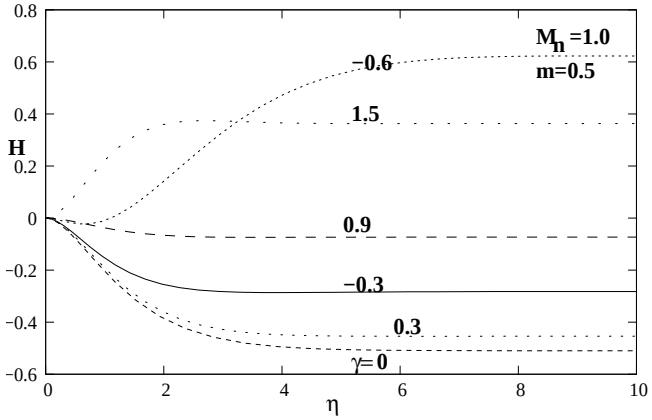

(c)

Figure 4. Velocity profiles of the generalized Von Kármán are shown for $M_n = 1.0$ and $m = 0.5$ at six different radial electric parameters, respectively in (a) for radial F, in (b) for tangential G, and in (c) for axial H components.

axial component of the velocity profiles decreases as Hall parameter increases. Above all, when the Hall parameter has a small negative value, H may become positive. Meanwhile,

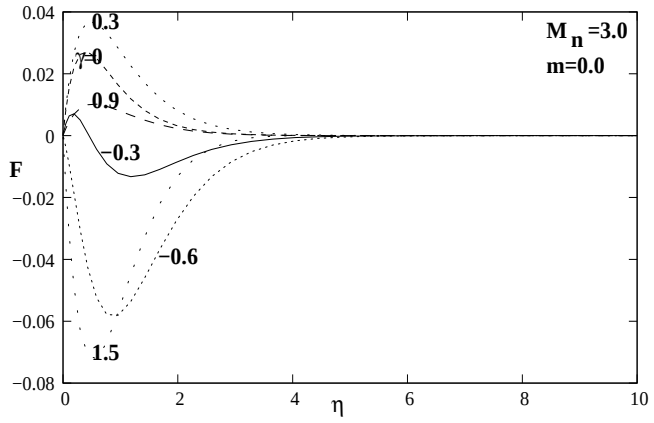

(a)

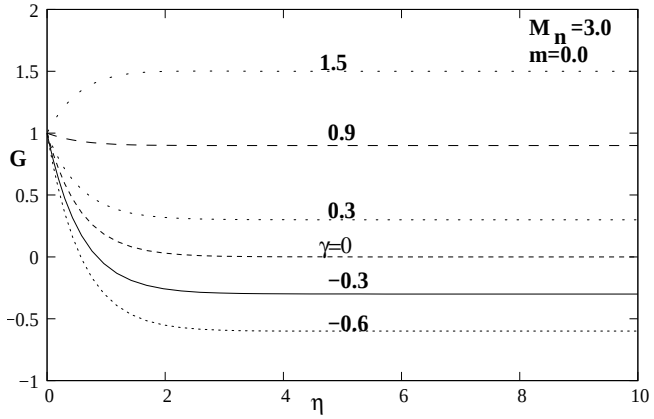

(b)

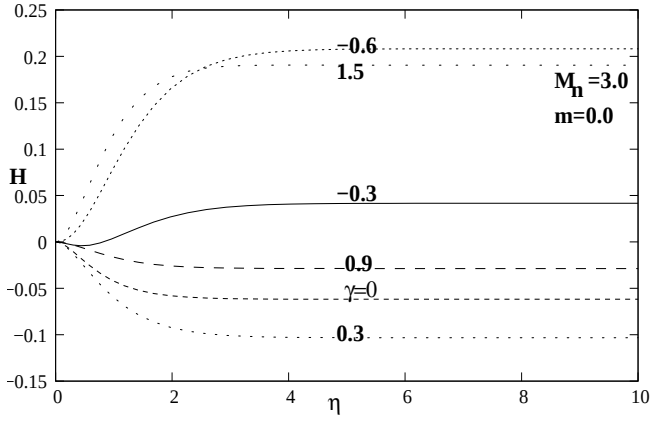

(c)

Figure 5. Velocity profiles of the generalized Von Kármán are shown for $M_n = 3.0$ and $m = 0.0$ at six different radial electric parameters, respectively in (a) for radial F, in (b) for tangential G, and in (c) for axial H components.

the impacts of magnetic interaction parameter are depicted in graphs(2(c)-7(c)). These

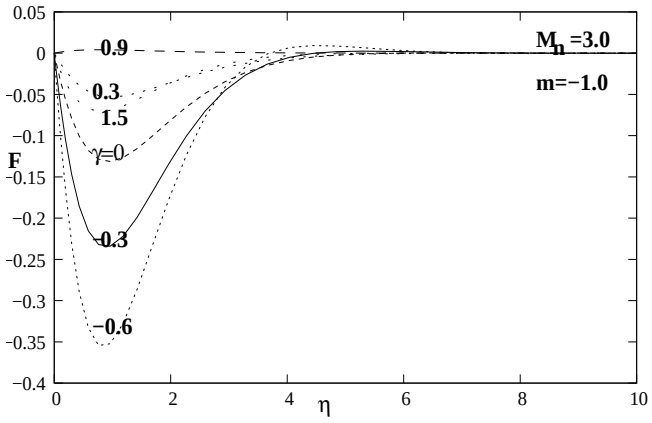

Figure 6. Velocity profiles of the generalized Von Kármán are shown for $M_n = 3.0$ and $m = -1.0$ at six different radial electric parameters, respectively in (a) for radial F, in (b) for tangential G, and in (c) for axial H components.

graphs demonstrate that the increment in the magnetic interaction parameter causes increment in the axial velocity values depending on positive electric parameters in radial

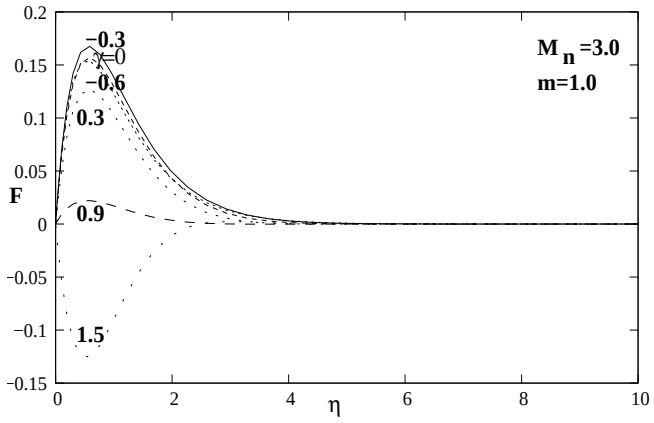

(a)

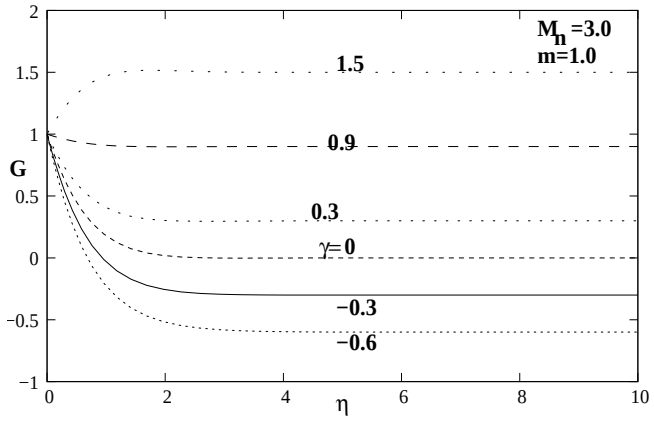

(b)

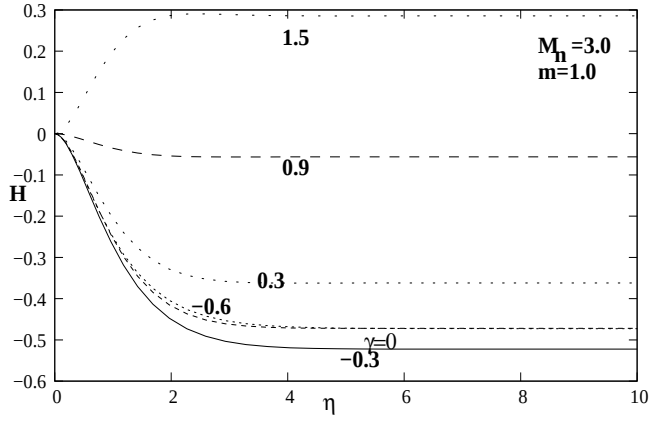

(c)

Figure 7. Velocity profiles of generalized Von Kármán are shown for $M_n = 3.0$ and $m = 1.0$ at six different radial electric parameters, respectively in (a) for F radial, in (b) for G tangential, and in (c) for H axial components.

direction and also depending on negative electric parameters in the same direction. All of these relations can be fairly seen in Table (3-4).

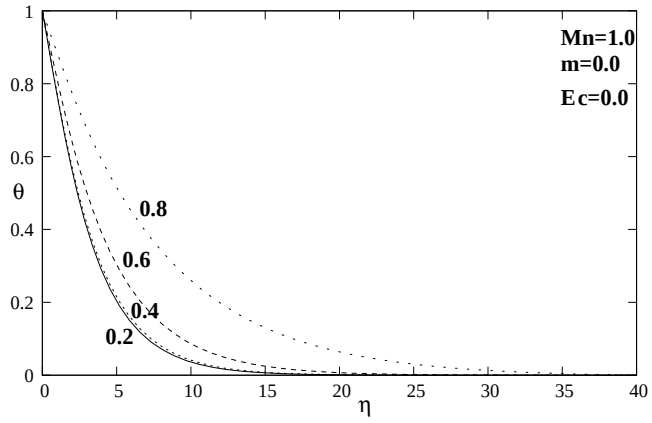

(a)

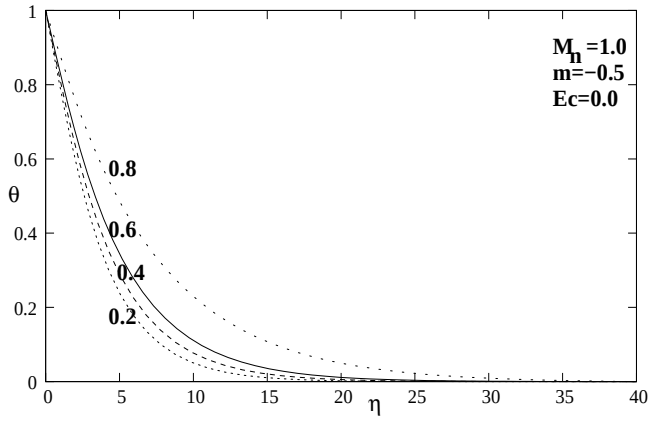

(b)

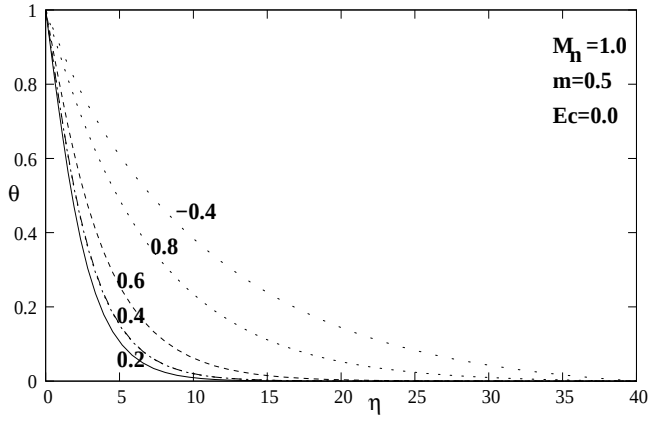

(c)

Figure 8. Temperature profile corresponding to heat transfer case is shown for $M_n = 1.0$ and $E_c = 0.0$ at different radial electric parameters respectively in (a) for $m = 0.0$, in (b) for $m = -0.5$, and in (c) for $m = 0.5$.

Temperature profiles, depending on the velocity components, are demonstrated in Figures(8-10), which are evaluated by using the equations (3.4-3.5) for different Eckert

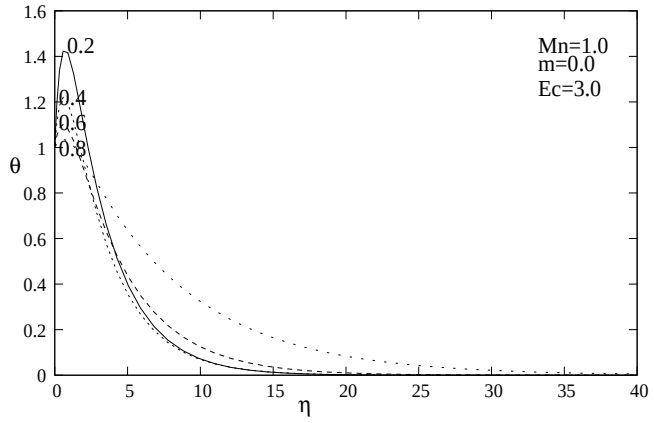

(a)

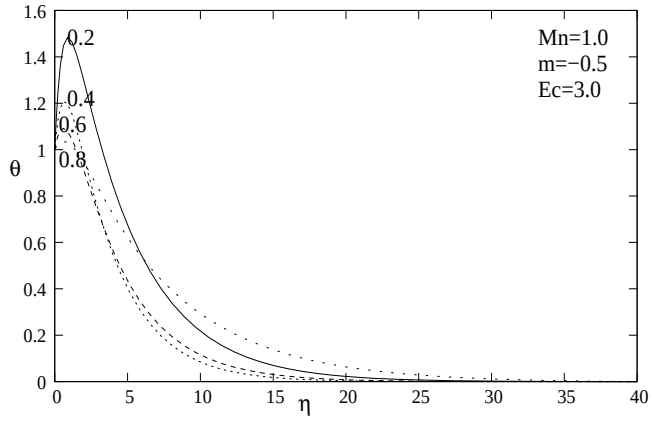

(b)

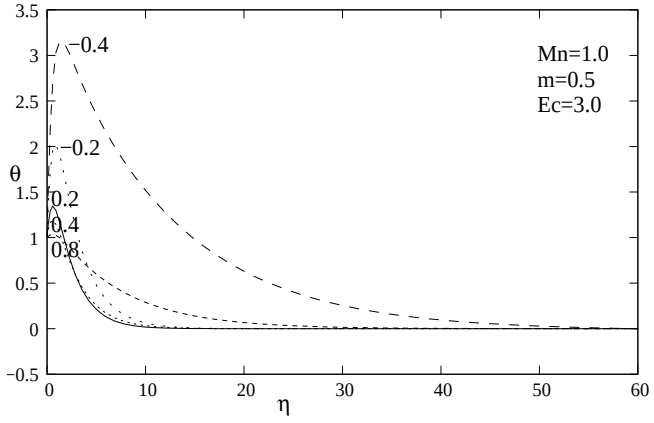

(c)

Figure 9. Temperature profile corresponding to heat transfer case is shown for $M_n = 1.0$ and $E_c = 3.0$ at different radial electric parameters respectively in (a) for $m = 0.0$, in (b) for $m = -0.5$, and in (c) for $m = 0.5$.

numbers, Hall parameters, magnetic interaction parameters with varying electric parameter in the radial direction at the fixed Prandtl number $P_r = 1.0$.

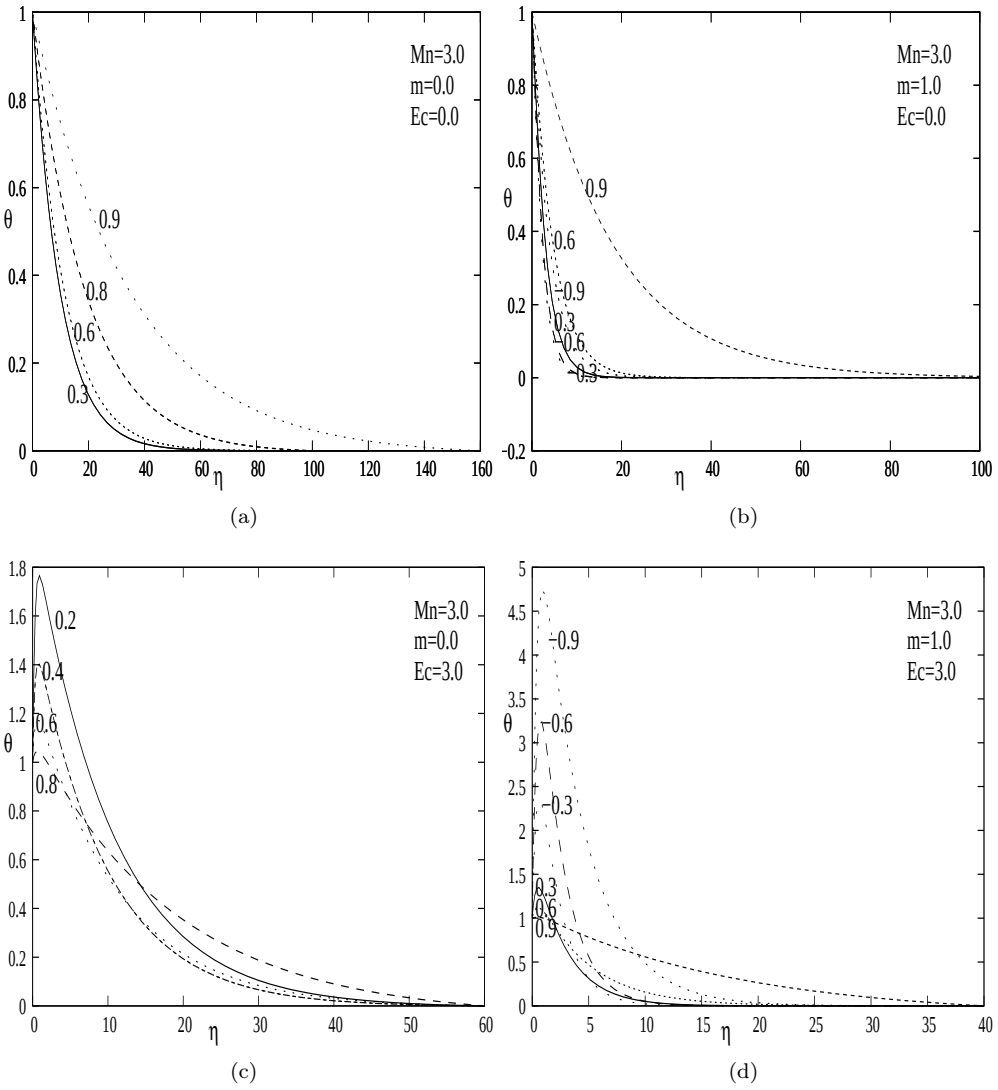

Figure 10. Temperature profile corresponding to heat transfer case is shown for $M_n = 3.0$ at different radial electric parameters respectively in (a) for $m = 0.0$, $E_c = 0.0$, in (b) for $m = 1.0$, $E_c = 0.0$, in (c) for $m = 0.0$, $E_c = 3.0$, and in (d) for $m = 1.0$, $E_c = 3.0$.

The effect of the Hall parameter is emphasized in Figures (8-10). It can be fairly inferred from the figures that for increasing Hall parameters the size of the interval of η shrinks, then this seems to occur for increasing Eckert numbers, as well. The case can also be observed easily for large magnetic interaction parameters. Furthermore, whenever Hall parameter increases, it is more temperature profiles are likely to be present for negative radial electric parameters. Table(5) also confirms the case, that is, the number of the presence of the more temperature profiles increases for the negative radial electric parameters.

It is also apparent from graphs (8) and (10) that when the Eckert number increases temperature profile increases too. Finally, the impacts of magnetic interaction numbers is given for increasing magnetic interaction numbers. As illustrated in Figures (8-10), the size of interval of η extends as magnetic interaction parameter increases.

Variations of the radial shear stress $F'(0)$, tangential shear stress $G'(0)$, the velocity in the radial direction $H(\infty)$ and coefficients of heat transfer $-\theta'(0)$ have been tabulated

M_n	m	γ	$F'(0)$	$G'(0)$	$H(\infty)$
1.0	-0.5	-0.6	-0.546781	-1.314478	2.707162
		-0.3	-0.102931	-1.113456	1.202871
		0.0	0.145142	-0.913193	9.205420E-002
		0.3	0.236486	-0.684928	-0.291948
		0.9	6.565356E-002	-0.111510	-7.689249E-002
		1.5	-0.457895	0.624115	0.403455
	0.0	-0.6	-0.112813	-1.538095	1.236077
		-0.3	0.170415	-1.315308	0.216396
		0.0	0.309257	-1.069053	-0.253314
		0.3	0.328034	-0.790558	-0.348514
		0.9	7.445934E-002	-0.125180	-6.913082E-002
		1.5	-0.489523	0.685647	0.361547
	0.5	-0.6	0.233191	-1.447853	0.621125
		-0.3	0.432856	-1.283261	-0.282036
		0.0	0.495221	-1.062616	-0.509727
		0.3	0.447946	-0.793985	-0.453959
		0.9	8.918274E-002	-0.126886	-7.328618E-002
		1.5	-0.554112	0.696890	0.363279

Table 3. Shear stress coefficients $F'(0)$ and $G'(0)$, vertical velocity $H(\infty)$ are tabulated at some chosen Hall parameters, radial electric parameters for fixed Magnetic interaction number $M_n = 1.0$.

M_n	m	γ	$F'(0)$	$G'(0)$	$H(\infty)$
3.0	-1.0	-0.6	-1.020161	-2.088827	1.243738
		-0.3	-0.640020	-1.649686	0.914910
		0.0	-0.338087	-1.241569	0.565473
		0.3	-0.124081	-0.858124	0.247915
		0.9	1.484372E-002	-0.123473	-1.746047E-002
		1.5	-0.226986	0.645086	0.275293
	0.0	-0.6	-6.191555E-002	-2.760873	0.208113
		-0.3	9.987538E-002	-2.254771	4.168429E-002
		0.0	0.190502	-1.747685	-6.176540E-002
		0.3	0.211255	-1.235386	-0.103263
		0.9	5.157919E-002	-0.180893	-2.865252E-002
		1.5	-0.358583	0.931506	0.190445
	1.0	-0.6	0.795771	-2.175726	-0.472718
		-0.3	0.805884	-1.834793	-0.522486
		0.0	0.734807	-1.462603	-0.472049
		0.3	0.590146	-1.059327	-0.361939
		0.9	0.104282	-0.161279	-5.608166E-002
		1.5	-0.612114	0.854623	0.285565

Table 4. Shear stress coefficients $F'(0)$ and $G'(0)$, vertical velocity $H(\infty)$ are tabulated at some chosen Hall parameters, radial electric parameters for fixed Magnetic interaction number $M_n = 3.0$.

for various radial electric parameter γ for the two different magnetic interaction numbers $M_n = 1.0$, $M_n = 3.0$, and Eckert numbers $E_c = 0.0$, $E_c = 3.0$ respectively in Tables (3-5). Because of increasing the Hall number m, the radial shear stress increases as the radial electric parameter gets less than unity. However, radial shear stress decreases when radial electric parameter gets larger than unity. It is apparent that reverse effect as a Magnetic interaction parameter is getting bigger.

M_n	E_c	m	$\gamma = -0.6$	$\gamma = -0.3$	$\gamma = 0.0$	$\gamma = 0.3$	$\gamma = 0.9$
1.0	0.0	-0.5	-	-	-	0.204831	8.911136E-002
		0.0	-	-	0.193041	0.239180	7.320891E-002
		0.5	-	0.222168	0.310924	0.294007	8.858441E-002
	3.0	-0.5	-	-	-	-1.086214	-2.805792E-002
		0.0	-	-	-2.661671	-1.250502	-2.820800E-002
		0.5	-	-4.106938	-2.312196	-1.162085	-3.069879E-002
3.0	0.0	-1.0	-	-	-	-	5.775309E-002
		0.0	-	-	8.285834E-002	0.107275	6.388499E-002
		1.0	0.319910	0.341921	0.322544	0.269701	7.936438E-002
	3.0	-1.0	-	-	-	-	2.106896E-003
		0.0	-	-	-5.020784	-2.411661	-2.226743E-002
		1.0	-8.848756	-5.836229	-3.493386	-1.762939	-3.213039E-002

Table 5. Heat transfer parameter $-\theta'(0)$ is tabulated at some chosen Hall parameters, radial electric parameters for the two different Magnetic interaction numbers $M_n = 1.0$, $M_n = 3.0$, and Eckert numbers $E_c = 0.0$, $E_c = 3.0$ respectively, and fixed Prandtl number $P_r = 1.0$.

Impact of Hall numbers on tangential shear stress can be deduced from these tables. It can be seen that the tangential shear stress increases in the case of increasing or decreasing Hall parameters values. In the event of the radial electric parameter becomes less than unity, when the magnetic interaction parameter increases the tangential shear stress decreases. On the other hand, if the radial electric parameter gets larger than unity, the effect on the shear stress in tangential direction becomes reversed.

5. Conclusions

The velocity and temperature profiles governing the steady-incompressible boundary layer flow over a rotating disk have been obtained using self-consistent assumptions. The resulting equations have then been solved numerically by using Chebyshev collocation method, and then the behavior of the velocity and temperature profiles are displayed graphically.

The effects of Hall parameter, radial electric parameter, Eckert parameter and magnetic interaction parameter are tabulated. One of the main outcomes of the present study is defining the effect of the Hall parameters on temperature profiles. This has been observed throughout for varying magnetic interaction parameters and radial electric parameters. Although the positive values of Hall parameter reveal the more temperature profiles for negative radial electric parameters, negative Hall parameter reverses the effect.

In this paper the effect of Hall parameter on the rotating disk is studied. Following this, we believe that, it would be interesting to study the effect of the electric field and also Hall parameter on instability mechanisms over rotating disk. For similar works, we refer to Jasmine &Gajjar [12] and Turkyilmazoglu [25]

Acknowledgment

I would like to express my deep appreciation for the referee's valuable contribution through their corrections and comments.

References

[1] Aboul-Hassan, A. L. and Attia, H.A. *The flow due to rotating disk with hall effect.* Phys. Lett. A **228**, 286-290, 1997.

[2] Attia, H.A. *Effect of Hall current on the velocity and temperature distributions of Couette flow with variable properties and uniform suction and injection.* Comput. Appl. Math. **28** (2), 195-212, 2009.

[3] Attia, H.A. and Ahmed, M. E. S. *Non-Newtonian conducting fluid flow and heat transfer due to a rotating disk.* ANZIAM J. **46** (2), 237-248, 2004.

[4] Attia, H. A., Ewis, K. M., Elmaksoud, I. H. A. and Awad-Allah, N. A. *Hydromagnetic rotating disk flow of a non-Newtonian fluid with heat transfer and ohmic heating.* J. Korean Soc. Ind. Appl. Math. **16** (3), 169-180, 2012.

[5] Benton,E. T. *On the flow due do rotating disk. Journal of Fluid Mechanics.* **24**, 781-800, 1966.

[6] Cess, R. D. *Unsteady heat transfer from a rotating disk to fluids with low Prandtl numbers in Applied Scientific Research* (Section A 1964).

[7] Cochran, W. G. *The flow due to rotating disk.* Proceeding of the Cambridge Philosophical Society, **30**, 365-375, 1934.

[8] Cramer, K. R., Bai S.and Pai. S. *Magnetofluid Dynamics for Engineers and Applied Physicists* (Scripta Publishing Company, 1973).

[9] Davies, D. R. *Heat transfer by laminar flow from a rotating disk at large Prandtl numbers.* Quart. J. Mech. Appl. Math. **12**, 14-21, 1959.

[10] Evans, H. L. *Laminar Boundary Layer Theory* (Addison-Wesley, 1968).

[11] Hossain, M. A., Hossain, A. and Wilson, M. *Unsteady flow of viscous incompressible fluid with tempreture-dependent viscosity due to a rotating disk in the presence of transverse magnetic field and heat transfer.* International Journal of Thermal Sciences, **40**, 11-20, 2001.

[12] Jasmine, H. A. and Gajjar, J. S. B. *Convective and absolute instability in the incompressible boundary layer on a rotating disk in the presence of a uniform magnetic field.* J. Engrg. Math. **52** (4), 337-353, 2005.

[13] Kármán, T. V." *Uber laminare und turbulente Reibung.* Zeitschnnift fur angewantee Mathematik und Mechanik. **1**, 233-252, 1921.

[14] Kumar, S. K., Thacker, W. I. and Watson, L. T. *Magnetohydrodynamic flow and heat transfer about a rotating disk with suction and injection at the disk surface.* Computers & Fluids **16** (2), 183-193, 1988.

[15] Millsaps, K. and Pohlhausen, K. *Heat transfer by laminar flow from a rotating plate.* J. Aeronaut. Sci. **19**, 120-126, 1952.

[16] Riley, N. *The heat transfer from a rotating disk.* Quart. J. Mech. Appl. Math. **17**, 331-349, 1964.

[17] Sahoo, B. *Effects of partial slip, viscous dissipation and Joule heating on Von Kármán flow and heat transfer of an electrically conducting non-Newtonian fluid.* Commun. Nonlinear Sci. Numer. Simul. **14**, 2982-2998, 2009.

[18] Schlichting, H. *Boundary Layer Theory* (McGraw-Hill, New York, 1968).

[19] Siddiqui, A. M., Rana, M. A. and Ahmed, N. *Effects of Hall current and heat transfer on MHD flow of a Burgers' fluid due to a pull of eccentric rotating disks.* Commun. Nonlinear Sci. Numer. Simul. **13** (8), 1554-1570, 2008.

[20] Sparrow, E. M. and Cess, R. D. *Magnetohydrodynamic flow and heat transfer about a rotating disk.* Trans. ASME Ser. E. J. Appl. Mech. **29**, 181-192, 1962.

[21] Sparrow, E. M. and Gregg, J. L. *Nonsteady surface temperature effects on forced convection heat transfer.* J. Aero. Sci. **24**, 776-777, 1957.

[22] Turkyilmazoglu, M. *Effects of uniform radial electric field on the MHD heat and fluid flow due to a rotating disk.* Internat. J. Engrg. Sci. **51**, 233-240, 2012.

[23] Turkyilmazoglu M. *A class of exact solutions for the incompressible viscous magnetohydrodynamic flow over a porous rotating disk.* Acta Mech. Sin. **28** (2), 335-347, 2012.

[24] Turkyilmazoglu, M. *The MHD boundary layer flow due to a rough rotating disk.* ZAMM Z. Angew. Math. Mech. **90** (1), 72-82, 2010.

[25] Turkyilmazoglu, M. *Resonance instabilities in the boundary-layer flow over a rotating disk under the influence of a uniform magnetic field.* J. Engrg. Math. **59** (3), 337-350, 2007.